Fusion Engineering and Design 161 (2020) 112061

Contents lists available at ScienceDirect

Fusion Engineering and Design

journal homepage: www.elsevier.com/locate/fusengdes

Improved reconstruction of JET using LIDAR-Vision fusion

Emil T. Jonasson [a,*], Jonathan Boeuf [b], Paul Murcutt [b], Stephen Kyberd [b], Robert Skilton [a]

[a] Cybernetics Department, RACE, UK Atomic Energy Authority, United Kingdom
[b] Oxford Robotics Institute, University of Oxford, United Kingdom

ARTICLE INFO

Keywords:
Remote maintenance
LIDAR
Kinematics
Reconstruction
Visual odometry
SLAM

ABSTRACT

Just like most industrial or scientific installations, future fusion reactors will require frequent maintenance. The expected environmental conditions and the necessity of carrying out many tasks in parallel result in the requirement to replace person-in-the-loop maintenance with robotic maintenance. Many advanced technologies will be required to carry out the automated inspection and maintenance tasks in order to minimize the maintenance shutdown durations. LIDAR is one such promising technology which is only just starting to be applied in Fusion contexts. Though it is presently not radiation tolerant enough to be utilized in future reactor designs such as ITER or DEMO without further development, the low radiation levels in JET have presented an opportunity to evaluate the technology for use in fusion environments. In previous work, we presented initial results using data captured in JET in the form of a coloured 3D-point-cloud created by LIDAR-Vision sensor fusion. In this paper, we present further work done to improve the quality of this data. This includes details on the improvement of model quality using ORB-SLAM as well as the use of recorded JET RH Boom kinematics data. We also carry out pointcloud-CAD data comparisons using numerical methods and show and improvement in reconstruction quality using ORB-SLAM and Boom Kinematics. Finally, the results are discussed and the relevance of this technology for future remote maintenance system inspection and navigation tasks is evaluated.

1. Introduction

The success of Nuclear Fusion as a cost-effective power source will be influenced strongly not just by the feasibility of the nuclear reaction itself, but also the cost-effectiveness of the maintenance operations required to keep the reactor running. For research reactors such as JET, the Joint European Torus (operated and maintained by the UK Atomic Energy Authority (UKAEA) on behalf of the EUROfusion consortium and located at the Culham Science Centre in Oxfordshire, UK), and ITER (under construction by Fusion 4 Energy in Cadarache, France) maintenance has been and will be carried out in a very person-intensive manner due to current limitations in technology. This is unlikely to be possible in future commercial fusion reactors due to the prohibitive costs and highly parallel maintenance operations required for cost-effective operation. Indeed, the commercial viability of the first demonstration reactor designed to be built in Europe, EU-DEMO, will be heavily dependent on high availability [1]. For this reason, the EU-DEMO reactor will require large numbers of robotic remote maintenance (RM) systems operating as autonomously as possible [2] in order to maximise availability whilst minimising the person-hours required to operate and supervise the equipment. These automated RM systems will be highly dependent on the sensor systems they use for navigation and inspection, and as such, this is an area which requires investigation.

One of the most promising currently available technologies for autonomous robotic navigation and inspection is LIDAR (LIght Detection And Ranging). If 3D-LIDAR data using mobile self-contained scanners can be collected successfully in a fusion context, this will vastly increase the capability of Fusion maintenance systems as long as radiation-tolerant mobile LIDAR scanners can be developed. For a short review of the current state of radiation hardening LIDAR systems, see [3].

1.1. Previous work

During the 2016/17 JET Maintenance Shutdown, the "NABU" sensor [4], was used to generate a metrology dataset of the inside of the JET torus. The NABU is a small, self-contained, portable surveying device

* Corresponding author.
E-mail address: emil.jonasson@ukaea.uk (E.T. Jonasson).

https://doi.org/10.1016/j.fusengdes.2020.112061
Received 22 September 2019; Received in revised form 12 October 2020; Accepted 12 October 2020
Available online 25 November 2020

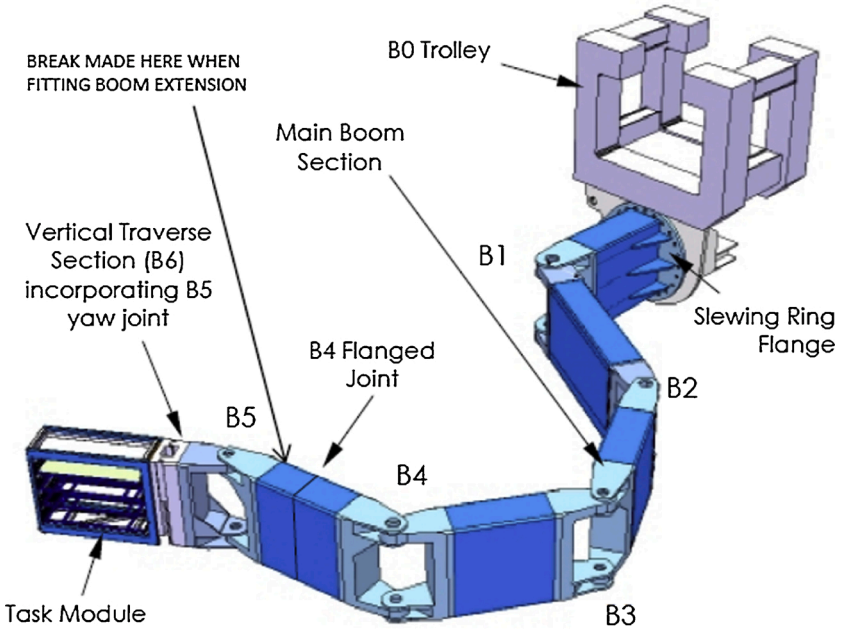

Fig. 1. Octant 1 Boom joints.

produced by the Oxford Robotics Institute (ORI), utilizing standard COTS Bumblebee X2 stereo camera, twin Hokoyu 2D-LIDAR scanners in a push broom configuration and two HD colour fisheye monocular camera. Using the Octant 1 Boom, the NABU was moved along the centre of the vessel as far in as the Oct 1' Boom was able to reach, starting with the right side of the vessel. After a 90 degree rotation of the NABU, the Boom then moved back to its starting position before moving into the left side of the vessel. The NABU was then turned back its original orientation, and the Boom once again moved to the starting position. Data collected included stereo and monocular visual and LIDAR point cloud data. At the same time, joint position data was collected from the Boom control system. A pointcloud was created by stitching together LIDAR scans. These were compared to the CAD models of the JET Vessel and were used to assess the basic feasibility of using these technologies for current and future RM applications such as mapping/inspection of components and localisation of automated RM systems [3].

1.2. Work presented in this paper

In this paper, we present further results obtained by processing and utilising the data collected in [3]. This includes details of the improvement in model quality using the ORB-SLAM method, as well as the use of co-recorded JET RM Boom kinematics for constructing an updated 3D-path for use in model re-construction. We carried out updated pointcloud-CAD data comparisons using numerical methods and produced histograms for comparison. The results of these comparisons are discussed with a view to the relevance of this technology for future remote maintenance system inspection and navigation tasks.

2. Improved pose estimation

The 3D-path originally generated by the NABU was not completely accurate due to drift in the dead-reckoning performed by the Visual Odometry (VO) using the on-board stereo camera. In addition, when creating the first reconstructions of the JET torus, data from the entire scan was used, even when passing over the same section twice. Due to the odometry drift between passes, this resulted in double walls appearing in the reconstruction. The drift due to the limitations of the VO can be corrected by using alternative methods such as ORB-SLAM [5], and by generating a more accurate 3D-path using angular sensor data from the Boom.

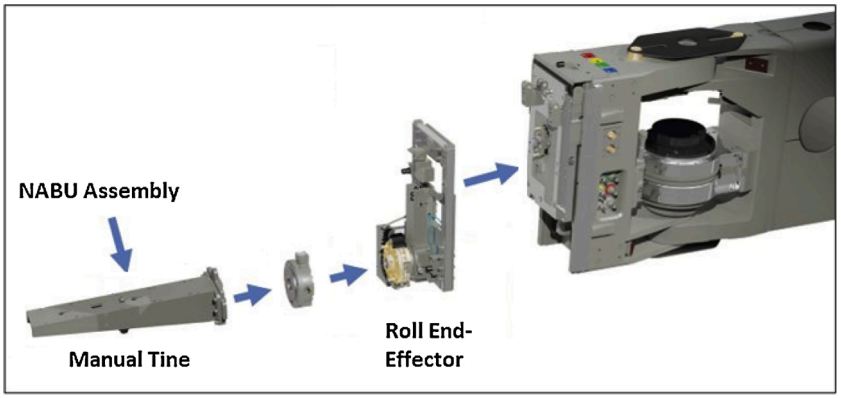

Fig. 2. Roll End-Effector and tine assembly. This replaces the Task Module shown on the end of the Boom in Fig. 1.

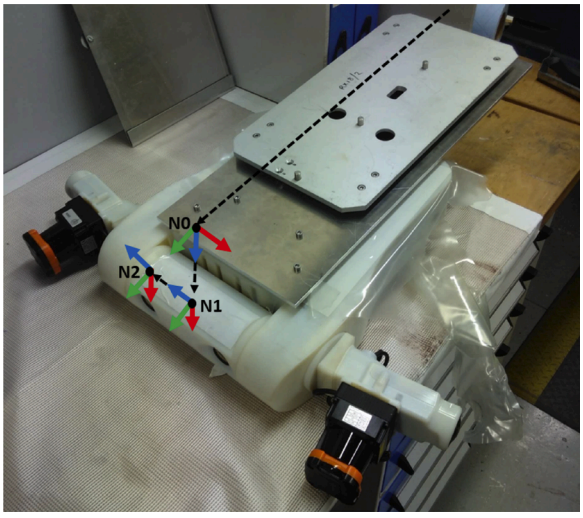

Fig. 3. NABU assembly. The light gray plate on the top comes from a Tile Carrier and attaches to the Manual Tine shown in Fig. 2, whilst the dark gray plate was manufactured specifically as a mounting adapter. Note that the assembly is pictured upside-down in this figure. DH-frames N0-N2 are detailed in this figure. Z = Green, X = Blue and Y = Red. (For interpretation of the references to colour in this figure legend, the reader is referred to the web version of this article.)

Table 1
Modified Denavit-Hartenberg parameters relating the centre of the NABU co-ordinate system to the Octant 1 Boom co-ordinate system.

Joint	θ_I	d_I	a_{i-1}	α_{i-1}
B_0	0	0	0	0
B_1	θ_1	0	$L0$	0
B_2	θ_2	0	$L1$	0
B_3	θ_3	0	$L2$	0
B_4	θ_4	0	$L3$	0
B_5	θ_5	0	$L4$	0
B_6	+90	0	L5	− 90
B_7	0	0	− $d6$	+90
N_0	θ_7	L_N	0	0
N_1	− 90	0	N_z	0
N_2	0	0	N_y	0

2.1. Boom transporter

The NABU was transported into the JET vessel using the "Tile Carrier Transfer Facility", also known as the "Octant 1 Boom", an 8 m long articulated transporter used to carry tools and materials into and out of the vessel as part of the JET RM system. The Oct 1 Boom is a serial manipulator with one prismatic "base" joint in the form of a trolley moving along a monorail ("B0") and five rotational joints forming the main structure ("B1-B5"). At the end of the Boom there is another prismatic joint which provides up-and-down movement in Z ("B6") and an attachment point for further end effectors to be installed.

The Task Module shown in Fig. 1 was removed, and the Boom was instead fitted with an end-effector called the "Roll End-Effector", which provides an additional rotational joint ("B7") allowing the payload to be oriented vertically or horizontally as required. The "Manual Tine" fits on the Roll End-Effector (Fig. 2) and enables the attachment of tooling such as Tile Carriers (not shown) for moving components into and out of the vessel. Using custom-made bracketry including a repurposed tile carrier plate (Fig. 3), the NABU was fitted to the Boom and carried into the JET vessel.

Table 2
Octant 1 Boom joint physical values.

Variable	Value
L_1	2415
L_2	1655
L_3	1660
L_4	1660
L_5	634
d_6	110
L_N	1008.45
N_z	61
N_y	60

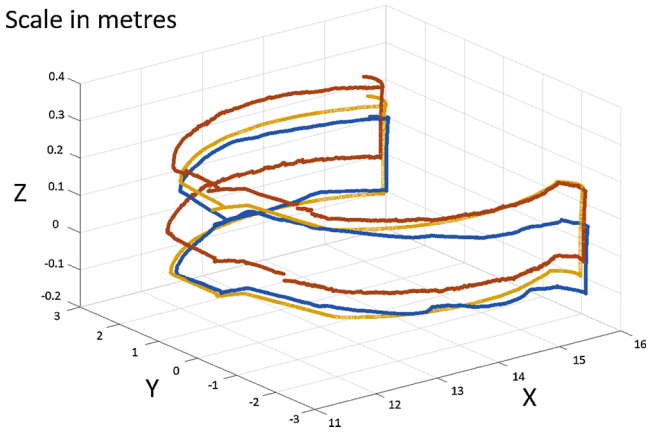

Fig. 4. VO in-vessel path in Blue, ORB path in Orange, Boom path in Yellow. The Boom carrying the NABU entered the vessel at approximately $X = 12$, $Y = 0$, $Z = 0$ (Refer to Fig. 5 for a reference on what each axis refers to in relation to the JET Vessel). Note scale on Z-axis is 1/10 of the scale on X and Y axes in order to highlight the (small) differences in height which the algorithms produce and to make the figure clearer. (For interpretation of the references to colour in this figure legend, the reader is referred to the web version of this article.)

2.2. Boom kinematics

Working out the kinematic equations to translate Boom joint angles to NABU sensor co-ordinates proved to be quite an undertaking due to the brackets and Roll-EE additions introducing a rotational joint with an offset in two axes. The NABU co-ordinate system origin was located inside the left stereo camera, and by measuring the offset from this origin to one of the attachment screw holes, and then to the B7/Roll End-Effector joint, the relationship between the Boom joint positions and the NABU co-ordinate system could be calculated.

The Boom joint kinematics parameters were then generated using the Modified Denavit-Hartenberg approach. B_1 to B_5 were assigned as co-ordinate frames relating to revolute and prismatic joints on the Boom itself, B_6 and B_7 relates to the Roll End-Effector, and finally N_0, N_1 and N_2 were the NABU co-ordinate frames assigned in the DH process of transposing the origin of the NABU from the centre of the left Stereo camera to the B7/R-EE joint. L_0 represents the prismatic joint position of joint B_0, and the rest of the variables have values as described in Table 2.

Once this was complete, Table 1 was used to generate the

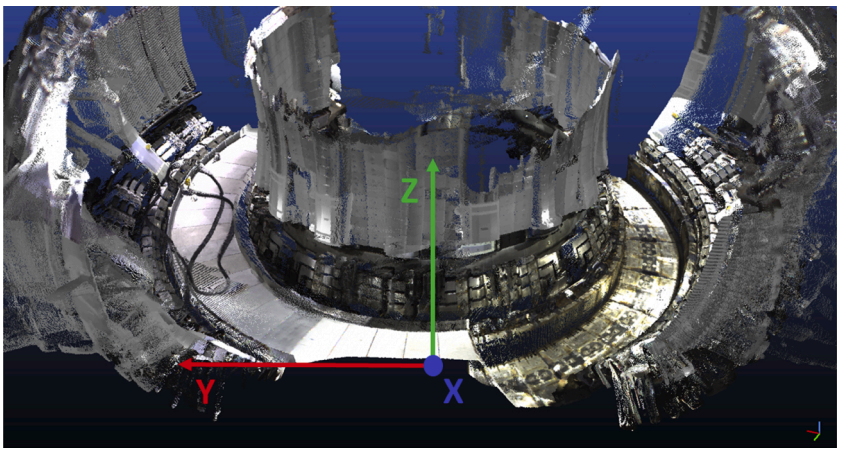

Fig. 5. Section of true colour pointcloud of JET vessel inner wall, reconstructed using Boom kinematics. Co-ordinate system marked in picture. In general terms, Z refers to the vertical axis of the Boom, X is the direction into the model as shown in this figure, and *Y* is the side-to-side movement. Refer to Fig. 4 for the path taken by the NABU. (For interpretation of the references to colour in this figure legend, the reader is referred to the web version of this article.)

transformation matrices between the Boom co-ordinate frame and the NABU frame for each and every joint in turn. Since these calculations necessitated the multiplication of eleven 4-by-4 matrices, an Octave script [6] using the Symbolic Mathematics Octave package [7] was written and used for this task. This was used to calculate a single transformation matrix which could be used with different joint angle combinations.

2.3. Boom 3D-path generation

When the kinematic equations of the Boom-NABU linkage had been determined, the resulting transformation matrix was populated with the values in Table 2. For each timestep, the recorded Boom Joint values (collected at the same time as the LIDAR measurements) were inserted into the transformation matrix. This was then used for calculating the XYZ-positions and Roll-Pitch-Yaw angles of the NABU co-ordinate frame at that timestep. This resulted in an updated 3D-path which was much more stable than the NABU-generated paths and did not suffer from dead-reckoning drift (see Fig. 4). All three data sources have the same starting position at (0, 0, 0). The Boom then travelled forward in X until it entered the vessel at about $X = 12$. The path is further described in Section 1.1. The figure also highlights the difference in Z (height) caused by the different approaches; however the scale of Z should be noted since it is an order of magnitude smaller than that in X and Y.

3. Data processing and analysis

3.1. ORB-SLAM

The original 3D-path of the sensor was calculated using Visual Odometry techniques similar to that used in [8]. ORB-SLAM, however, offered the opportunity to improve the quality of the odometry by utilising a Simultaneous Localisation And Mapping approach, localising against previously visited places thus reducing the accumulation of drift in the VO. We ran the ORB-SLAM2 algorithm [5] over the Bumblebee stereo image data with the default ORB-SLAM2 vocabulary and 2000 features per image.

3.2. Reconstruction

Using the newly created 3D-paths, software developed in-house by ORI using techniques similar to [9] was used to stitch together the 2D-scan slices into a 3D-pointcloud of the inside of the JET vessel. The timestamped 2D LIDAR slices were placed in 3D-space in the appropriate XYZ locations along the 3D-path. The points were assigned a colour using the data from the monocular cameras, resulting in a coloured 3D-pointcloud.

3.3. Model comparison

During maintenance Shutdowns, the JET RH Operations Team maintain a Configuration Model which reflects the state of the JET vessel during the maintenance shutdown period. This is updated as components are added or taken away. The CAD model used for the comparison was generated from the Configuration Model for the day of the data collection and exported as an.STL file. The open source software program CloudCompare [10] was used to subsample this model with 10 000 points, creating a new pointcloud which was smaller and easier to work with. The reconstructed pointclouds were first manually aligned to the sampled CAD by carrying out 180° or 90° rotations as necessary to align the co-ordinate systems, and finally moving the measured clouds along the X-axis (axes as shown in Fig. 4) to align the scan starting positions with each other. CloudCompare's ICP (Iterative Closest Point) algorithm was used to carry out the final alignment. CloudCompare's Cloud-to-Cloud distance comparison function was then used (using standard settings apart from the selection of a quadric surface model, the most accurate but slowest option) and the resulting scalar field was displayed as histograms of distances.

4. Results

The results of this work are presented here. An example section of one of the pointclouds generated from the reconstruction process is shown in Fig. 5. This shows the fine detail of the inner wall of the JET Torus which has been captured by the NABU device. Pointclouds of the entire scan were used for comparison with the JET CAD, and the histograms in Fig. 6 show the results (as an absolute distance measurement) of a comparison of each reconstruction type with a sub-sampled pointcloud of the JET CAD. Finally, comparing the reconstruction produced using the Boom kinematics approach and the JET CAD model (without subsampling) produced a heatmap, a section of which can be seen in Fig. 7.

5. Discussion

The results show a definite improvement over the Visual

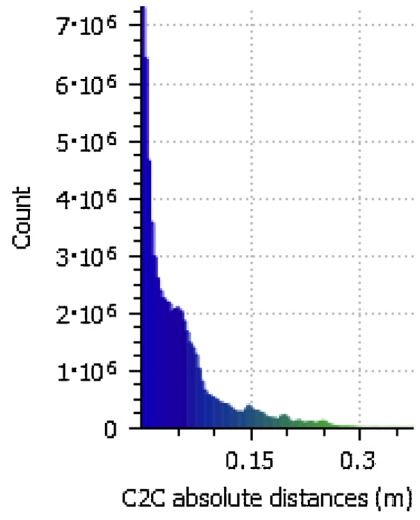

(a) Visual Odometry

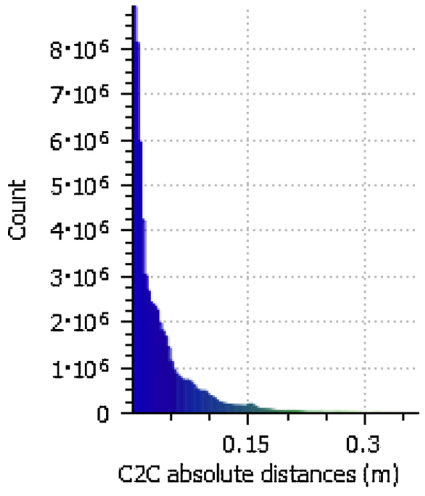

(b) ORB-SLAM

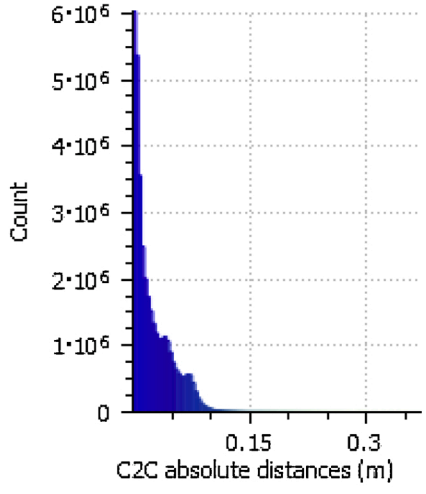

(c) Boom Kinematics

Fig. 6. Histograms of Cloud-to-Cloud ("C2C") comparisons between NABU LIDAR pointclouds and sub-sampled JET CAD data. (a) Visual Odometry results (pointcloud generated as part of [3]); (b) Pointcloud generated using ORB-SLAM; (c) Pointcloud generated using Boom Kinematics.

Odometry approach when using ORB-SLAM or Boom Kinematics (Fig. 6). That being said, this work has also shown that the approaches using sensor input from the NABU alone for the 3D-path reconstruction (VO and ORB-SLAM) have performed very well given the non-standard use case and (in the case of the VO) the reliance on what is essentially a dead-reckoning process for localisation. The differences in the Histograms are clear but in each case, the vast majority of points are within a few millimetres of the CAD model, indicating good performance from all reconstruction methods. Outliers with values of up to 0.5 m can be seen in Fig. 7 but the number of these points are so small that they are not even visible in the Histograms in Fig. 6. They seem to be related to measurement equipment mounted in the Vessel during the Shutdown.

It is possible that the gradual decline in Z-value (on the order of about 10 cm) which can be seen in both the VO and ORB-SLAM 3D-paths in Fig. 4 as the Boom and Scanner moved towards the "right-hand" side of the vessel (when entering the vessel from Octant 1) in the VO and ORB-SLAM reflects the reality of the Boom "drooping" slightly as it is extended due to its own weight and the effect of gravity. Since the Boom lacks any on-board capacity to measure this, it works on a theoretically flat X-Y plane. However, it is also possible that this drooping is caused by the gradual drift of the Z-estimate for both VO and ORB-SLAM as the NABU progressed further into the vessel – especially since the rotations carried out at the end of each movement falls into the category of a "challenging camera movement" according to the OSB-SLAM paper [5]. That this drift exists in some fashion can be seen in the different Z-values of the lines in Fig. 4 at $X = 11$, $Y = 0$, despite the fact that the Z-values started off at 0 in each approach. Refer to [3] for a description of the movements the Boom (and hence NABU) made before entering the Vessel. This is likely the reason that the Boom kinematics data showed the lowest absolute distance error when compared to the CAD.

One of the problems encountered during the processing was the alignment of the reconstruction pointclouds with the CAD model, since the three reconstructions all produced pointclouds aligned with slightly different co-ordinate systems. It is possible that accurately aligning them using ICP placed the pointclouds in slightly different positions compared to the CAD for evaluation, which may have affected the results.

6. Conclusion

In this paper, we have produced an improved 3D-reconstruction of the inside of the JET Vessel. We have compared the use of three different techniques for this task, one being the use of Stereo Visual Odometry used in our previous work, one being the ORB-SLAM algorithm (using only data collected by the NABU sensor), and the final method utilising information both from the LIDAR and Camera data collected by the NABU as well as from the Boom joint sensors themselves. We aligned the pointclouds with the CAD models of the JET vessel and evaluated the differences between the measurements and reality. Comparing the histograms, there is a clear improvement in the distribution of distances using ORB-SLAM and Boom Kinematics, with the latter showing the best result. It has a large number of values (roughly one third of the total) within the sub-mm range, further demonstrating the suitability of LIDAR as an inspection tool in Fusion once the radiation hardness challenges are overcome. In addition, there is a clear qualitative improvement of the reconstruction quality, allowing easy identification of a range on in-vessel components by visual inspection.

Potential future work includes further model quality improvement, segmentation of the vessel interior into tiles and other components, detection of specific component location discrepancies between the CAD model and the dataset, and use of data for live or simulated live Boom localisation using registration such as in [11].

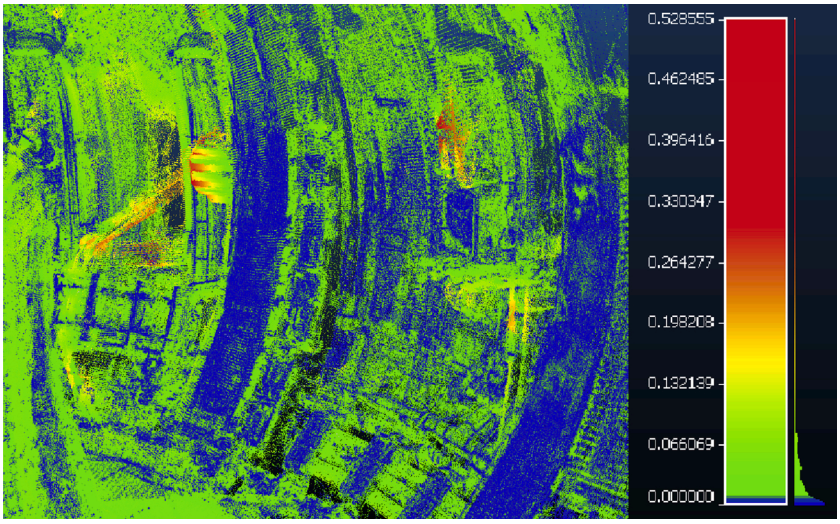

Fig. 7. Heatmap of outer vessel wall (left-hand side of Fig. 5) showing Pointcloud-CAD distances using Boom data, scale in metres. Outliers over 0.15 m are shown in orange and red. (For interpretation of the references to colour in this figure legend, the reader is referred to the web version of this article.)

Declaration of interests

None declared.

Declaration of Competing Interest

The authors report no declarations of interest.

Acknowledgments

The authors would like to thank EUROfusion for the opportunity to carry out this research. Emil Jonasson would like to thank John Blackburn for development of the system for kinematic data collection from the JET RH System, and Matthew Goodliffe for invaluable assistance with kinematics calculations. In addition, the authors would like to thank the developers of the *Symbolic Math* toolbox for Octave, which was utilised extensively for the matrix multiplications for the kinematics.

This work has been carried out within the framework of the EUROfusion Consortium and has received funding from the Euratom research and training programme 2014–2018 and 2019–2020 under grant agreement No 633053. The views and opinions expressed herein do not necessarily reflect those of the European Commission.

Stephen Kyberd, Paul Murcutt, Jonathan Boeuf and Robert Skilton have received funding from UK Research and Innovation and EPSRC through the Robotics and Artificial Intelligence for Nuclear (RAIN) research hub [EP/R026084/1].

References

[1] D. Maisonnier, I. Cook, S. Pierre, B. Lorenzo, B. Edgar, B. Karin, D.P. Luigi, F. Robin, G. Luciano, H. Stephan, N. Claudio, N. Prachai, P. Aldo, T. Neill, W. David, The European power plant conceptual study, Fusion Eng. Des. 75–79 (2005) 1173–1179, https://doi.org/10.1016/j.fusengdes.2005.06.095, proceedings of the 23rd Symposium of Fusion Technology.

[2] J. Thomas, A. Loving, C. Bachmann, J. Harman, DEMO hot cell and ex-vessel remote handling, Fusion Eng. Des. 88 (9) (2013) 2123–2127, https://doi.org/10.1016/j.fusengdes.2013.02.080. Proceedings of the 27th Symposium On Fusion Technology (SOFT-27); Liège, Belgium, September 24–28, 2012.

[3] E.T. Jonasson, J. Boeuf, S. Kyberd, R. Skilton, G. Burroughes, P. Amayo, S. Collins, Reconstructing JET using LIDAR-Vision fusion, Fusion Eng. Des. (2019) 110952, https://doi.org/10.1016/j.fusengdes.2019.03.069.

[4] Oxford Robotics Institute: Survey Equipment, 2019. https://ori.ox.ac.uk/application/survey.

[5] R. Mur-Artal, J.D. Tardós, ORB-SLAM2: an open-source SLAM system for monocular, stereo and RGB-D cameras, IEEE Trans. Robot. 33 (5) (2017) 1255–1262, https://doi.org/10.1109/TRO.2017.2705103.

[6] J.W. Eaton, D. Bateman, S. Hauberg, R. Wehbring, GNU Octave Version 4.4.1 Manual: A High-Level Interactive Language for Numerical Computations, 2019. https://www.gnu.org/software/octave/doc/v4.4.1/.

[7] Symbolic-Octave Symbolic Package Using SymPy(version 2.7.0), 2019. https://octave.sourceforge.io/symbolic/.

[8] D. Nister, O. Naroditsky, J. Bergen, Visual odometry, Proceedings of the 2004 IEEE Computer Society Conference on Computer Vision and Pattern Recognition, 2004, CVPR 2004, vol. 1 (2004), https://doi.org/10.1109/CVPR.2004.1315094. I.

[9] A.D. Stewart, P. Newman, Laps-localisation using appearance of prior structure: 6-dof monocular camera localisation using prior pointclouds, 2012 IEEE International Conference on Robotics and Automation (2012) 2625–2632, https://doi.org/10.1109/ICRA.2012.6224750.

[10] CloudCompare (Version 2.9.1), 2018. http://www.cloudcompare.org/.

[11] S. Ruel, T. Luu, M. Anctil, S. Gagnon, in: Target Localization From 3D data for On-Orbit Autonomous Rendezvous & Docking, IEEE, 2008, pp. 1–11, https://doi.org/10.1109/AERO.2008.4526516.